Computers & Geosciences 86 (2016) 1–14

Contents lists available at ScienceDirect

Computers & Geosciences

journal homepage: www.elsevier.com/locate/cageo

Case study

Development of a visualization tool for integrated surface water–groundwater modeling

Yong Tian [a,b], Yi Zheng [b,*], Chunmiao Zheng [a,b,c]

[a] School of Environmental Science and Engineering, South University of Science and Technology, Shenzhen 518055, Guangdong Province, China
[b] College of Engineering, Peking University, Beijing 100871, China
[c] Department of Geological Sciences, University of Alabama, Tuscaloosa, AL 35487, USA

ARTICLE INFO

Article history:
Received 6 April 2015
Received in revised form
23 September 2015
Accepted 24 September 2015
Available online 9 October 2015

Keywords:
Scientific visualization
GSFLOW
Integrated surface water–groundwater modeling
Heihe River Basin
Water resources management

ABSTRACT

Physically-based, fully integrated surface water (SW)-groundwater (GW) models have been increasingly used in water resources research and management. The integrated modeling involves a large amount of scientific data. The use of three-dimensional (3D) visualization software to integrate all the scientific data into a comprehensive system can facilitate the interpretation and validation of modeling results. Nevertheless, at present few software tools can efficiently perform data visualization for integrated SW–GW modeling. In this study, a visualization tool named IHM3D was designed and developed specifically for integrated SW–GW modeling. In IHM3D, spatially distributed model inputs/outputs and geo-referenced data sets are visualized in a virtual globe-based 3D environment. End users can conveniently explore and validate modeling results within the 3D environment. A GSLFOW (an integrated SW–GW model developed by USGS) modeling case in the Heihe River Basin (Northwest China) was used to demonstrate the applicability of IHM3D at a large basin scale. The visualization of the modeling results significantly improved the understanding of the complex hydrologic cycle in this water-limited area, and provided insights into the regional water resources management. This study shows that visualization tools like IHM3D can promote data and model sharing in the water resources research community, and make it more practical to perform complex hydrological modeling in real-world water resources management.

1. Introduction

In recent years, due to the rapid growth of computing capacity, physically-based, fully integrated surface water (SW)–groundwater (GW) models have been increasingly used in water resources research and management. These models can provide a spatially and temporally detailed description of basin-scale hydrologic cycle, and simulate a variety of state and flux variables (Maxwell et al., 2014). Some representative models include GSFLOW (Coupled Ground-Water and Surface-Water Flow Model) (Markstrom et al., 2008), HydroGeoSphere (Brunner and Simmons, 2012), MIKE-SHE (Graham and Butts, 2005), ParFlow (Srivastava et al., 2014) and PAWS (Shen and Phanikumar, 2010). Integrated SW–GW models have been used to address various water and environmental issues, such as land use and climate changes (Gilfedder et al., 2012; Markstrom, 2012; Maxwell and Kollet, 2008), SW–GW interactions (Hassan et al., 2014; Huntington and Niswonger, 2012) and irrigation management (Condon and Maxwell, 2013; Pérez et al., 2011; Wu et al., 2015).

Integrated SW–GW modeling requires a great amount of data, especially for large river basins with significant heterogeneity. Typical data requirements include Digital Elevation Model (DEM), soil, land use, meteorological data and others used for model setup, as well as streamflow and groundwater head measurements and others used for model calibration and validation. With recent science and technology developments, many new data types are available for the modeling, such as remote sensing (RS) products of rainfall (Kühnlein et al., 2014), evapotranspiration (ET) (Rasmussen et al., 2014), soil moisture (Hirschi et al., 2014) and Leaf Area Index (LAI) (Hu et al., 2014), as well as outputs from other physically based models like regional climate models (Xiong et al., 2009). On the other hand, integrated SW–GW models often produce gigabytes of output data that are both spatially distributed and temporally variant. Therefore, an integrated SW–GW model is not only a simulation tool, but also a platform for data integration (Tian et al., 2015b). Efficient and informative graphic displays of the large amount of modeling data are highly desired to aid process

* Corresponding author.
E-mail address: yizheng@pku.edu.cn (Y. Zheng).

http://dx.doi.org/10.1016/j.cageo.2015.09.019
0098-3004/

interpretation and management decision making.

Modern visualization techniques like three-dimensional (3D) GIS (Castrillón et al., 2011), Graphics Processing Unit (GPU) programming (Lázaro et al., 2014) and virtual globes (Wu et al., 2010; Liu, et al., 2015) are frequently used to develop various 3D visualization tools. The technique of virtual globes has become popular in the field of environmental and natural resources (Mochales and Blenkinsop, 2014; Zhu, et al., 2014). A 3D virtual globe presents geographical information in a way that perceives the 3D aspects of geographical features, and therefore provides a more realistic perception of the actual environment. Google Earth (Jacobson et al., 2015), NASA World Wind (Boschetti et al., 2008) and ArcGlobe (Shojaei et al., 2013) are the most commonly used virtual-globe tools. These tools all support the representation of various location-aware contents including images, points and 2D/3D shapes, etc. As they were designed for general purpose, additional programming efforts are necessary for developing domain-specific applications. For example, Google Earth has been used as the platform to develop visualization tools for meteorological data (Chen et al., 2009; Wang et al., 2013). Nevertheless, applications specifically for integrated hydrological models are still rare.

In hydrology and geoscience communities, many 3D visualization tools have been developed (Bernardin et al., 2011; Brooks and Whalley, 2008; Castrillón et al., 2011; Li et al., 2013; McCarthy and Graniero, 2006) which could be used to present the data involved in integrated SW–GW modeling. But few of them are able to conveniently handle the diverse data types involved in the modeling and efficiently visualize them. In addition, many of the existing tools do not display data in a geo-referenced environment, and therefore it is hard to display the data within background environments (e.g., terrain, landscape, sunlight, etc.). Other generic Geographic Information System (GIS) tools, such as Google Earth and Esri's ArcScene and ArcGlobe, have more powerful visualization capacities. But they have not been specifically designed for hydrological studies, and cannot easily process the data of integrated SW–GW models. For example, when presenting time series of spatially distributed data, both Google Earth and ArcScene use key-frames to represent significant states to be shown in the frames. The frames have to be created by users on their own.

To fill the gap discussed above, we designed and developed a visualization tool, IHM3D (IHM stands for Integrated Hydrological Modeling), specifically for integrated SW–GW modeling, which can display geo-referenced data sets in a virtual 3D environment. It can animate time series of data fields (e.g., ET, soil moisture, groundwater level, overland flow, etc.) on a virtual globe. Well-implemented graphic functions (e.g., zooming, panning, flying, rotation, lighting, rendering, etc.) are also provided. When developing the software, we considered the data structure of GSFLOW. GSFLOW is a typical integrated SW–GW model which has been applied in many studies (Hassan et al., 2014; Huntington and Niswonger, 2012; Markstrom, 2012; Surfleet et al., 2012; Wu et al., 2014). A video demo of IHM3D is available at http://yun.baidu.com/s/1dDrrvvr.

2. System design and implementation

2.1. The integrated model

GSFLOW was developed by USGS (Markstrom et al., 2008), which integrates the surface hydrology model PRMS (Bae et al., 2011; Leavesley et al., 1983) with the classic groundwater flow model MODFLOW. It performs 2D surface hydrology simulation and 3D groundwater simulation. Hydrologic response units (HRUs), either regular grid cells or irregular polygons, are the basic computing units in PRMS. The subsurface domain is discretized into finite difference girds in MODFLOW. GSFLOW defines “gravity reservoir” as a storage in which a HRU exchanges water with the MODFLOW grid(s) it intersects. In GSFLOW, a vadose zone between the soil zone and the aquifer is conceptualized and modeled by the Unsaturated Zone Flow package (UZF1) (Niswonger et al., 2006). Streams and lakes are simulated using the Streamflow Routing package (SFR2) (Niswonger and Prudic, 2010) and Lake package (LAK3) (Merritt and Konikow, 2000), respectively. Stream-aquifer exchanges are calculated based on the head difference between a reach and the subsurface grid cell(s) it intersects, using Darcy's law. More details about GSFLOW and its components can be found in Markstrom et al. (2008). Some model improvements were conducted by Tian et al. (2015a), and our study used this improved version.

A variety of data are required to establish a GSFLOW model. For example, a DEM is used to define surface topology, top elevations of MODFLOW grids, as well as streambed elevations; soil type and land cover maps are used to determine HRU types and their associated model parameters; stream and aqueduct networks are needed to define the drainage system; meteorological data are used as forcing functions; and streamflow and groundwater head observations are required for model calibration and validation. GSFLOW's outputs cover all the major state variables and fluxes of basin-scale hydrologic cycle. The model inputs and outputs can both be 3D data (3D in space, or 2D in space plus the time dimension) or 4D data (3D in space plus the time dimension). Typical 3D data include ET, average soil moisture, hydrogeological parameters (e.g., specific yield), meteorological data (e.g., precipitation); and typical 4D data are groundwater heads. In IHM3D, all 3D/4D data are stored in the HDF5 format (http://www.hdfgroup.org/HDF5/), which is a widely adopted format for storing and organizing large amounts of numerical data.

2.2. System design

Fig. 1 illustrates the design principles of IHM3D. The software system renders a 3D virtual globe of the Earth, and users are able to freely move around in the virtual 3D environment and view scientific data associated with the integrated model. Data layers are the fundamental mechanism to display information in the system. Each layer references a dataset and specifies how that dataset is portrayed. Data layers in IHM3D can be classified into five categories (Fig. 1). The first is a base terrain layer which presents the 3D terrain surface derived from DEM data. Other spatially referenced data can be displayed on top of it. The second category is GIS layers which present standard vector and raster data. The third is model layers used to present model inputs and outputs, including model spatial structures (e.g., computational grids, subsurface cross-sections, drainage systems, pumping well locations, etc.), distributed parameters (e.g., soil features, hydrogeological properties, river characteristics, etc.), driving forces (e.g., meteorological data), and model simulation results. IHM3D can display the model inputs and outputs in their original data formats, without transforming them into standard GIS data formats. The fourth is a layer of point observations which displays time-series observations (e.g., streamflow and temperature at gaging stations, groundwater head at monitoring wells, etc.) achieved at specific locations. The final category is 3D-object layers displaying static 3D objects (e.g., buildings, trees, etc.), which provide more realistic views.

IHM3D uses WGS84 (World Geodetic System 1984) as the basic coordinate system. Any layers to be visualized in IHM3D have to be transferred to this coordinate system. The project transformation is automatically performed by IHM3D, as long as the original project information is available. In addition, all the layers should contain their altitude information. The layers can obtain this

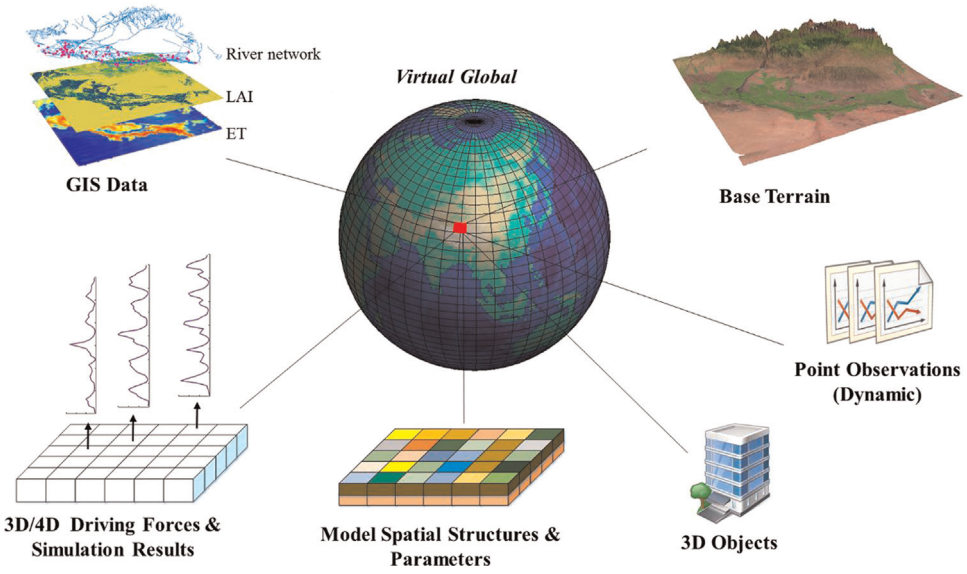

Fig. 1. Design principles of IHM3D.

information from themselves or from the base terrain layer.

Fig. 2 illustrates the architecture of IHM3D. The architecture uses a three-tier approach which is common to modern software. The data tier in the bottom contains different data sources. The data sources could be remote data servers distributed on the Internet, local files, and local databases. In this system, elevation data and satellite images (e.g., Landsat images) for rendering base terrain are dynamically retrieved from remote servers (e.g., global elevation data server maintained by NASA) via standard Open Geospatial Consortium (OGC) protocols including Web Map Service (WMS) and Web Feature Service (WFS) (Michaelis and Ames, 2012). The local data files include GIS data files, model inputs and output files, time series observations at specific points and 3D object files. The retrieved data from remote data servers are cached in the Local Database to improve the terrain rendering performance. The Local Database is implemented based on popular relation databases (e.g., Microsoft SQL Server, SQLite, etc.), which provide high performance for data query and management. Point time series in different file formats (e.g., Excel format.xlsx,.txt and. csv) can also be imported and saved in the Local Database. Storage of the time-series data follows a standard observational data template called Observations Data Model (ODM) (Horsburgh et al., 2008). ODM provides a generic database template to store hydrologic observations and metadata about the data values, and has been widely used within the hydrology community (Horsburgh and Reeder, 2014; Peckham and Goodall, 2013; Huang and Tian, 2013; You et al., 2014).

The middle tier forms the backbone of the system. The 3D rendering engine encapsulates key algorithms to emulate realistic 3D environments (e.g., landscape, atmosphere, sky, etc.) and visualize scientific data. Particularly, the classic Level of Detail (LOD) algorithms (Lindstrom et al., 1996) are applied to render the 3D base terrain. For better performance, the elevation data and images are saved in the Local Database, and organized into tiled structures based on LOD algorithms. It also provides a real-time camera control for navigation in the virtual environment. The Data Manager is responsible for communicating with the diverse data sources in the bottom tier. ADO.NET and SQLite-Net that provide access to relation databases are used. Two third-party libraries, DotSpatial and HDF5DotNet, are employed to manipulate standard GIS data and HDF5 data. The Plug-in Manager enables the system to locate and load available extensions. It relies on a plug-in mechanism through which the system can expose itself and consume external plug-ins. The Cache Manager determines which data

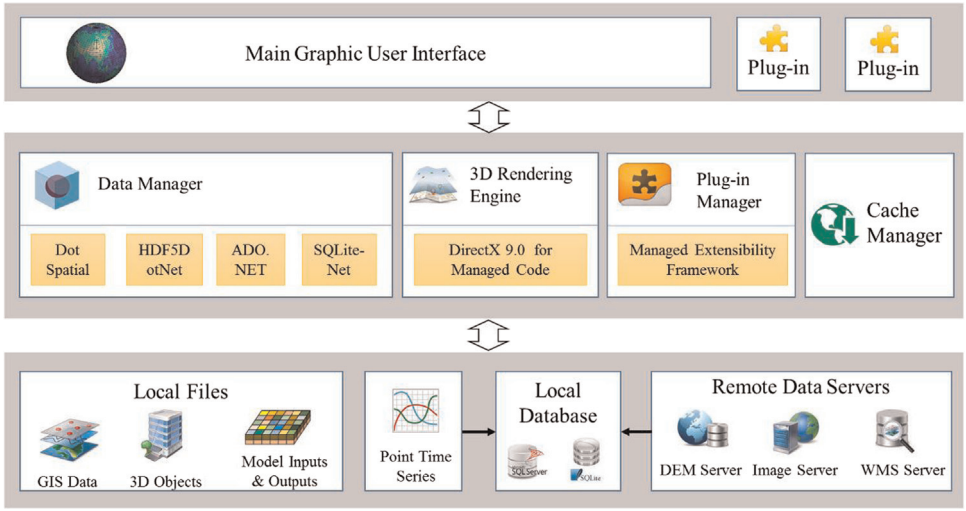

Fig. 2. System architecture of IHM3D.

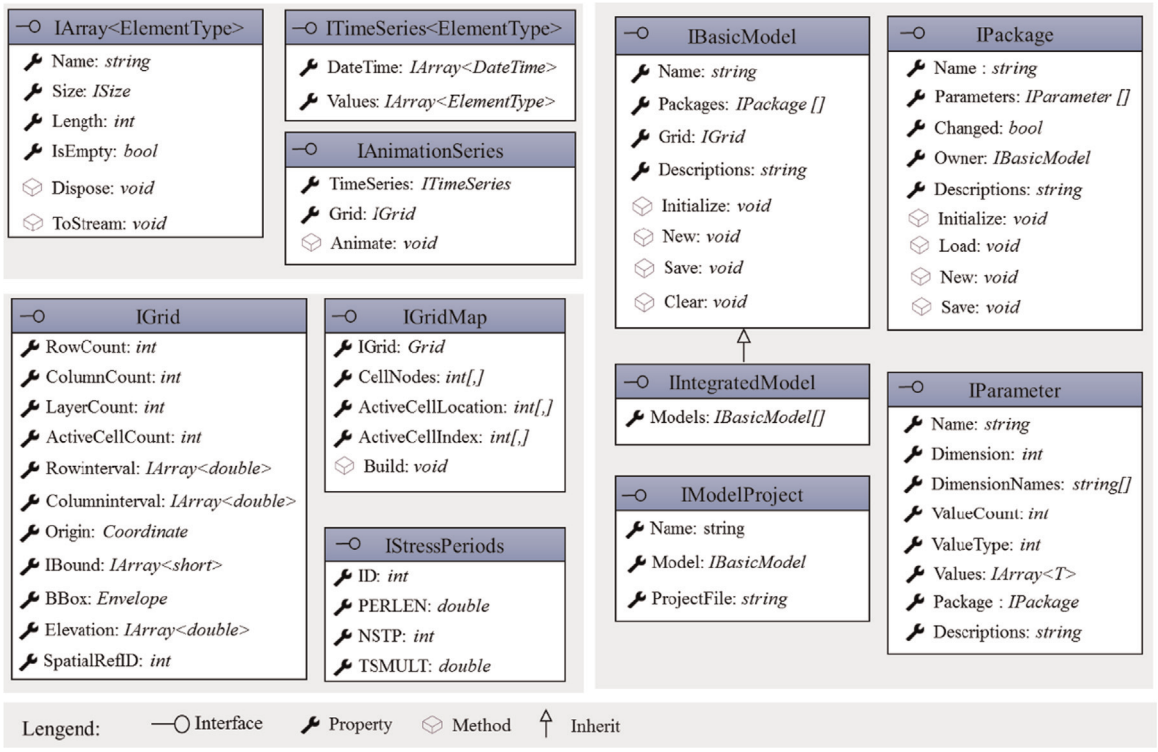

Fig. 3. Design of core data structures in IHM3D.

should be retrieved from remote servers and how the retrieved data would be organized and stored in the Local Database.

The top one is the presentation tier, which handles user interactions via graphic user interface (GUI). The main GUI provides an interactive geo-referenced environment in a global view. It provides the users with an integrated view for data interaction, real-time access to online data, data mashup and visualization. The main GUI also enables to accept plug-ins to extend its capabilities. Many useful utilities provided by the system are offered by means of plug-ins. The default plug-ins include a time series viewer that can plot time series data as line graphs, and an animation player that can control animation playing.

To effectively handle various data types associated with an IHM, a standard data structure to encapsulate computational arrays has been designed. Fig. 3 depicts the core interfaces in the data structure. IArray < T > represents generic interfaces which can hold elements of arbitrary inner type (usually numerical system types like *double* or *int*). The arrays encapsulated by IArray < T > can have any dimension numbers to represent scalars, vectors and matrices. It provides flexibility for creating sub-arrays and altering existing data, and makes it much easier to perform loops, initialization and other tedious tasks. The ITimeSeries interface was designed for holding time-series data of multiple variables. The *IGrid* interface describes the rectangular computational units (i.e., grid cells) of an IHM. Its *Origin* property is the coordinates of the upper-left grid cell. Its *IBound* property designates each cell as active, active with constant head, or inactive. The IGridMap interface provides the index information of grid cells. The IAnimationSeries defines animation operations performed on the Grid, the animated data source is defined by the *TimeSeries* property. The IStressPeriods interface describes computational time intervals for MODFLOW simulation. The IBasicModel, IIntegratedModel, IModelProject, IPackage and IParameter interfaces together describe an IHM. The IBasicModel represents a numerical model, its *Packages* property describes the packages owned by the model. The IIntegratedModel inherited from the IBasicModel specially describe the IHM consisting of several models. The IPackage defines a package thatcontains a set of parameters. All the parameters are represented by the IParameter. The IModelProject contains meta-data about the IHM. These five interfaces together capture common attributes and behaviors of models.

2.3. System implementation

2.3.1. Programming languages

IHM3D was developed using the C# language based on Microsoft.NET Framework (Version 4.5). The.NET Framework provides several unique components which greatly facilitate the development, including Managed Extensibility Framework (MEF), Windows Presentation Foundation (WPF), and Language Integrated Query (LINQ). MEF allows.NET applications to discover and use extensions without configuration. With MEF, the problem of fragile hard dependencies, often encountered in developing extensible applications, could be avoided. WPF is Microsoft's latest solution to delivering rich and interactive experiences for desktop applications. Compared with the traditional GUI solution using WinForms, WPF has many unique features. It supports extensible application markup language (XAML), 2D and 3D graphics, animation, styles, data binding and other graphical control elements that are essential for application developers. It enables developers to include rich elements and animations in applications with greatly reduced workload. LINQ is a technique for querying data. It is fully integrated into.NET languages like C#, which makes it much easier to query and update data of different source types in developing data-extensive applications like IHM3D.

2.3.2. Project management

IMH3D uses a project file to store metadata about an IHM, the file is an Extensible Markup Language (XML) based document. It consists of two sections: one stores the metadata about a particular integrated SW–GW model (e.g., model name, path of model

master file, etc.), and the other stores the metadata about data layers. The system provides a management tool to deal with creation and modification of the project file.

2.3.3. 3D rendering engine

The 3D rendering engine was developed by leveraging Microsoft DirectX 9.0 for managed code. DirectX 9.0 provides a set of low-level application programming interfaces (APIs) for creating high-performance 3D graphics applications. The 3D rendering engine uses a forward rendering pipeline to display layers. How the 3D rendering engine handles different data layer types is described below:

2.3.3.1. Base terrain layer. The classic quadtree LOD technique was used to generate and visualize 3D terrain surface. The LOD technique is able to keep up the appearance of the scene as realistic as possible, while reducing the graphic complexity (Castrillón et al., 2011; Lindstrom et al., 1996; Suárez and Plaza, 2009). When the user navigates over the terrain, the system would display the most favorable mesh representation, in terms of the distance terrain-observer. High-resolution satellite images are used as textures on wire-frame of the mesh. During the navigation process, satellite imagery and elevation data are dynamically retrieved from remote data servers, such as i-cubed Landsat7 Imagery server and global elevation data server maintained by NASA. Remote data retrieval, caching and clean algorithms implemented by the Caching Manager component manage the quadtree in real time.

2.3.3.2. GIS layers. DotSpatial library (http://dotspatial.codeplex.com/) was utilized to incorporate GIS data and analysis into IHM3D. DotSpatial supports a variety of GIS data types and provides functionalities for manipulating and analyzing GIS data. It has been increasingly used recently for developing scientific tools (Ames et al., 2012; Horsburgh and Reeder, 2014; Osna et al., 2014; Steiniger and Hunter, 2013). Since DotSpatial is an open-source GIS library and is completely developed using C#, it can be easily incorporated in software based on.NET platform. With DotSpatial, vector data encoded in Shapefile and Keyhole Markup Language (KML) formats can be displayed in the 3D environment. Raster data can also be directly loaded and draped on top of the base terrain.

2.3.3.3. Model layers. To visualize model inputs and outputs, the system first loads model input files and establishes spatial structures of the model (i.e., model grids, stream network, etc.). Values of other model inputs and outputs can then be visualized and animated based on the model structures. For the subsurface domain, IHM3D adopts a 2.5D approach to display subsurface data layer by layer horizontally, and cross-section by cross-section vertically. As the integrated SW–GW modeling is usually implemented in a large area (e.g., thousands of square kilometers), this 2.5D approach not only provides a higher rendering efficiency, but also makes the data interpretation more convenient.

2.3.3.4. Point observations layer. This layer stores the locations of observational sites. Through this layer, time-series observations at specific locations can be presented in terms of chart plots.

2.3.3.5. 3D objects layers. Static 3D objects encoded in *.x* format can be loaded and displayed in IHM3D. Users are asked to specify locations and scales of each 3D object. 3D objects should be created in other 3D modeling software (e.g., SketchUp, 3D Studio Max etc.,) before they are loaded into IHM3D.

2.3.4. Graphic user interface (GUI)

The main GUI of IHM3D (Fig. 4) consists of interactive elements including pull down menus, tree lists and toolbars. Additional elements (e.g., scale bar, compass, legend bar, etc.), in the form of child windows floating on the base map, can be turned on/off as needed. Once the system is started, a virtual globe is lunched, and a base terrain map is presented. The base terrain map can use Landsat7 image as the base imagery. The system can display elevation data and satellite images at varying levels of detail. Users can manipulate the globe, view data in a global view and then seamlessly zoom in to visualize detailed and localized data.

While opening the project file, the model and data layers referred by the file will be loaded into the system through a lazy loading mode. Only visible layers will be initialized and presented on the virtual globe. A layer manager organizes the loaded layers in a tree-like structure. Users can specify presentation style (e.g., color, opacity, etc.) of layers. Users are also allowed to add or delete a layer, toggle a layer's visibility, or set a layer's transparency. If model layers are turned on, users can quickly and easily browse

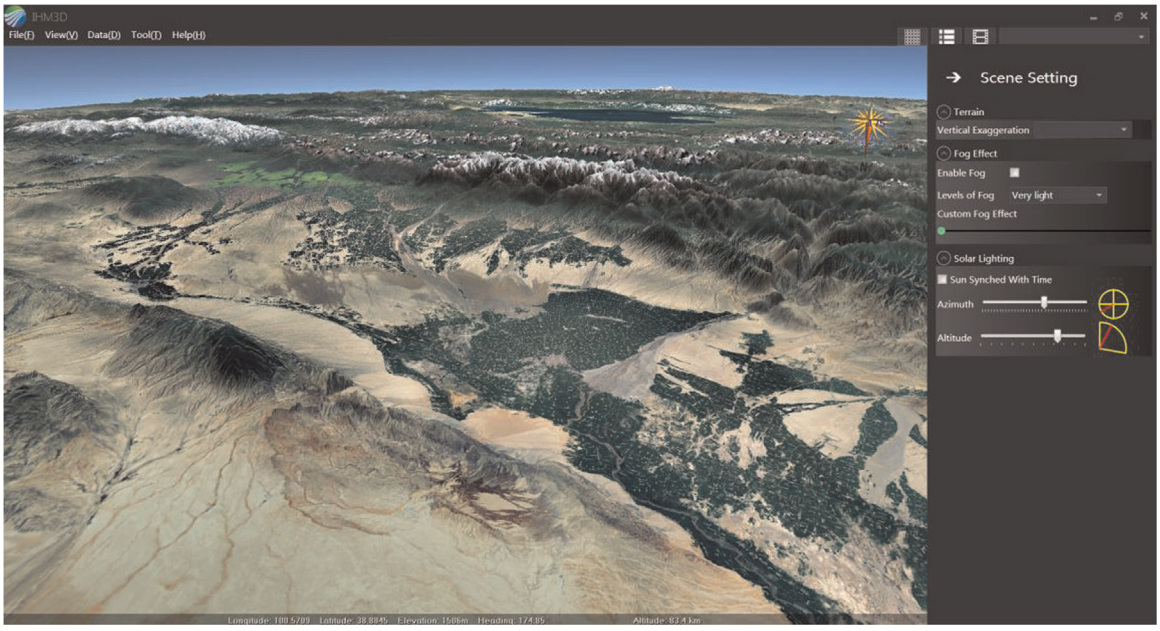

Fig. 4. Main graphic user interface of IHM3D.

the model's spatial structures, animate model output variables, and probe data values of model parameters and output variables.

3. System application

3.1. Application case

The Heihe River Basin (HRB) is the second largest endorheic river basin in China. It is one of most water-stressed basins in China. Overexploitation of water resources has caused a number of ecological problems and social conflicts in HRB, including reduction of environmental flow to the Gobi Desert area in the downstream, disappearance of wetlands, soil salinization and vegetation degradation. Recently, integrated SW–GW modeling by GSFLOW has been conducted for the middle and lower HRB, which helps understand the complex hydrological processes and improve the regional water resources management (Tian et al., 2015a, 2015b; Wu et al., 2014, 2015). A powerful 3D visualization tool like IHM3D would further enhance the value of the modeling for the management.

Our system application case is based on the GSFLOW model of HRB established by Tian et al. (2015b). The modeling domain (Fig. 5) consists of the entire middle and lower HRB and a west portion of the Badain Jaran Desert whose groundwater system is hydraulically connected with HRB. It is bounded by the Qilian Mountains on the south, the Badain Jaran Desert on the east and the Mazongshan Mountains on the west, covering a total area of 90,589 km^2. The domain contains three distinctive parts, the middle HRB, the lower HRB and the west portion of the Badain Jaran Desert. The middle HRB has many alluvial fans and floodplains along the mountain foot, as well as intensively irrigated farmlands in oases. The annual average temperature is about 8 °C, and the annual average precipitation is about 145 mm. The lower HRB is a vast Gobi-desert area. The vegetation mainly develops in the floodplain areas along the river. The annual average temperature and precipitation are about 10 °C and less than 50 mm, respectively. The desert part has tall stationary dunes and numerous scattered lakes (probably fed by groundwater) (Jiao et al., 2015). The annual average temperature is about 9 °C, and the annual precipitation is below 110 mm.

The integrated model was run at a daily time-step from January 1, 2000 to December 31, 2012, with the first year as a "spin-up" period. For streamflow, the model calibration period was from 2001–2008, and the left 4 years were the validation period. For groundwater level, the data length is shorter, and the calibration was performed for 2001–2005, and the validation for 2006–2007. The model calibration was manually accomplished in a trial-and-error manner. More details about the model setup, calibration and validation can be found elsewhere (Tian et al., 2015b).

3.2. Visualization of data for model setup, calibration and validation

To build, calibrate and validate the integrated model, tremendous data have been collected. All the data were provided by the Heihe Program Data Management Center (http://www.heihedata.org). The data used for model setup and initial parameterization include DEM, land use, soil type and hydrogeology map, borehole data, stream network and aqueduct network. Some of them are displayed in Fig. 4. The stream network contains more than 30 perennial rivers which bring over 3.5 billion m^3 per year surface runoff from the Qilian Mountains to the middle HRB. Nearly half of the surface runoff is delivered by the main Heihe River through Yingluoxia, which is the dividing point between the upstream and midstream. Zhengyixia divides the midstream and downstream. At Langxinshan, the main river diverges into the East River and the West River, which drain the flow into the East and the West Juyan Lakes, respectively. In addition, four major

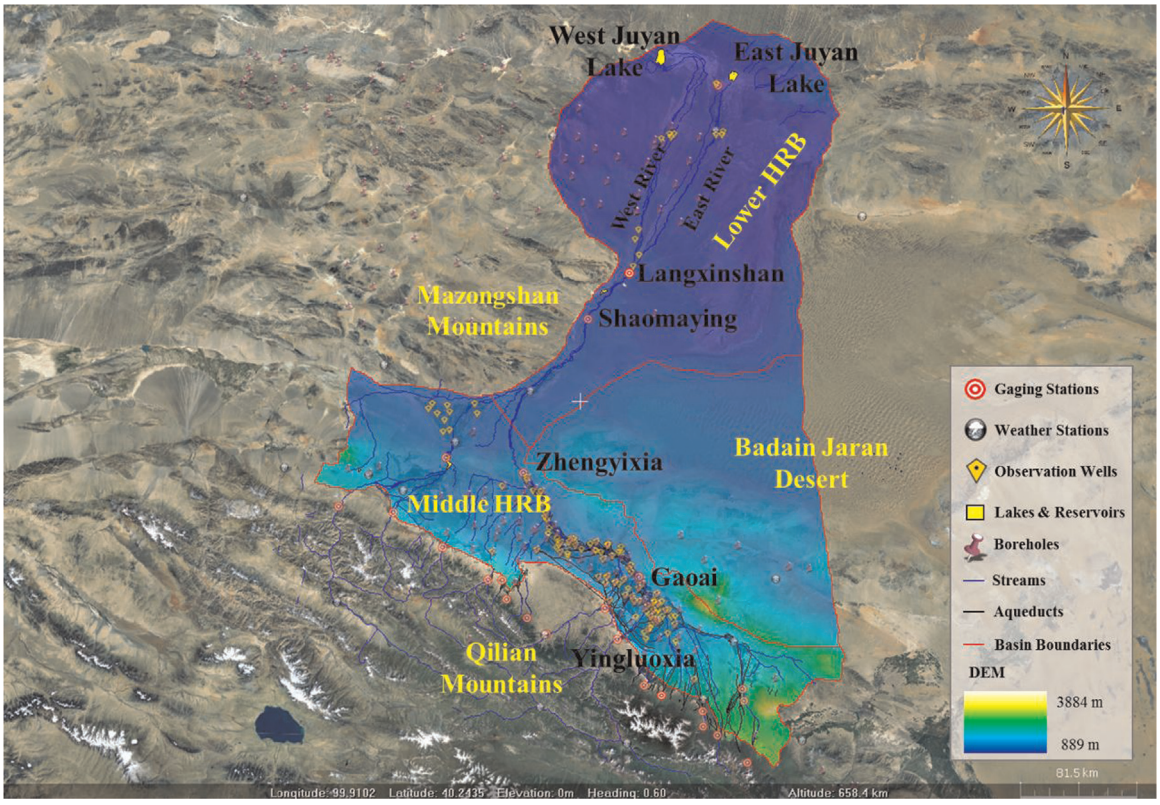

Fig. 5. The case study area displayed in IHM3D.

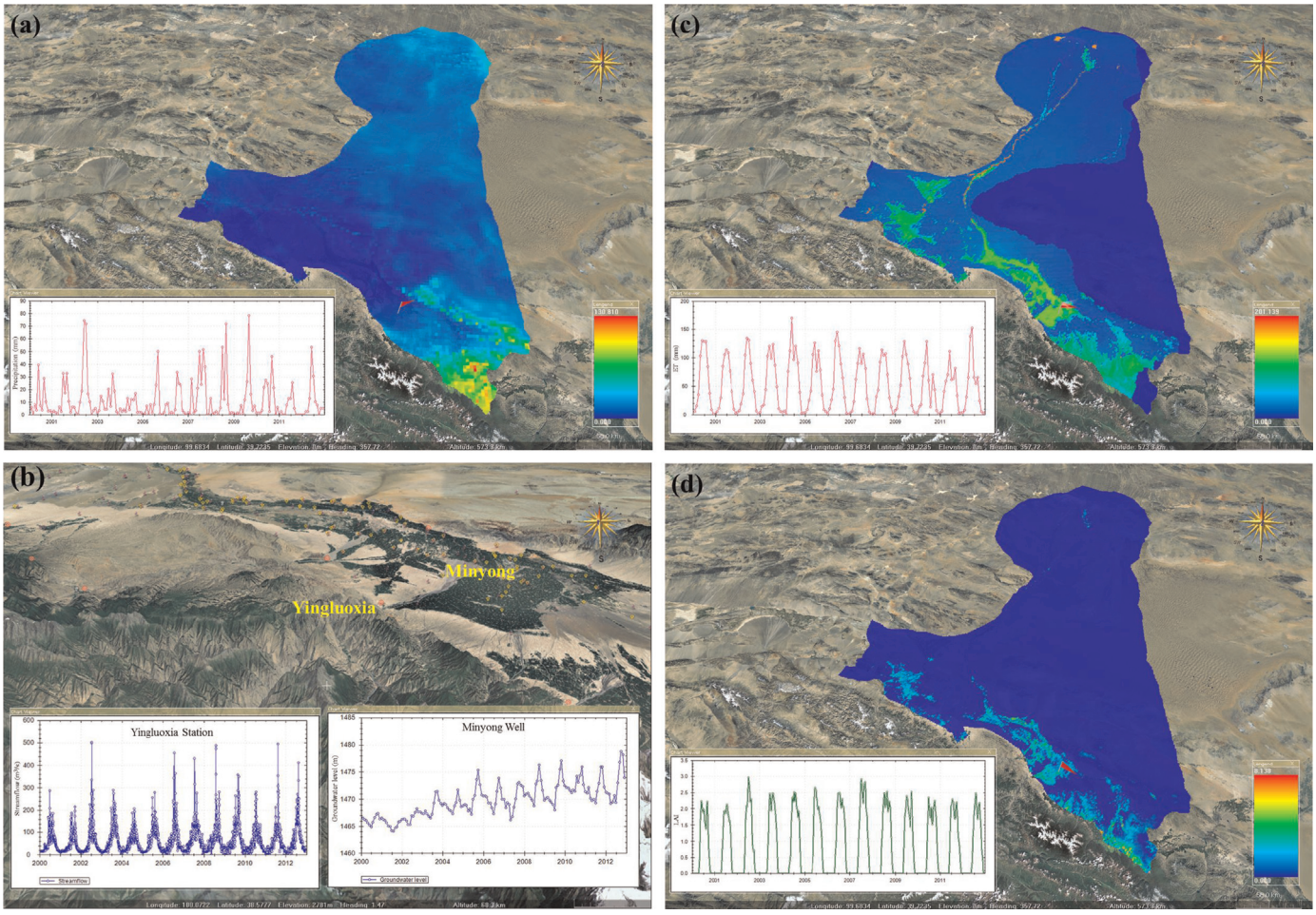

Fig. 6. Data for model setup, calibration and validation. (a) Precipitation field; (b) daily streamflow at Yingluoxia and monthly groundwater level at Minyong Station; (c) remote sensing-based evapotranspiration (ET) data; and (d) remote sensing-based Leaf Area Index (LAI) data. (For interpretation of the references to color in this figure, the reader is referred to the web version of this article.)

reservoirs and two terminal lakes (yellow polygons), as well as the locations of 257 boreholes (pins), are also illustrated.

Meteorological data are the key forcing functions for the model. Within or adjacent to the modeling domain, only 19 weather stations (Fig. 4) maintain long time-series and high quality weather observations. Alternatively, meteorological data produced by a regional climate model (Xiong and Yan, 2013) (3 km × 3 km grids) were used, including precipitation, temperatures (maximum, minimum and average), relative humidity, wind speed and wind direction. Fig. 6a displays the spatial distribution of precipitation on a specific day. The chart view in Fig. 6a presents the dynamics of monthly precipitation at a selected location (indicated by the red flag). In fact, users can view the dynamics at any locations with data available. By selecting a location of interest, a pop-up context menu appears to guide the user to retrieve the time-series data. Allowing for extracting values at locations of interest help the user better diagnose the modeling results, but existing tools usually do not offer such convenience. Other dynamic inputs, such as boundary surface inflows, surface water diversion rates and groundwater pumping rates, can be visualized in the same way. IHM3D can also produce animations to show the temporal variation of data fields like the precipitation field. Existing tools such as ArcScene and Google Earth use key-frames to represent the significant states to be shown in the frames, which have to be created by users on their own. IHM3D can directly produce animations without defining key-frames by users. In the application case, streamflow observations at 4 gaging stations and groundwater level observations at 47 monitoring wells (Fig. 4) were used to constrain the model simulation. After right-clicking an observational point, a pop-up menu with basic information about that point will appear, from which a chart view of time-series observations can be shown. As an example, in Fig. 5b, the observed daily streamflow at the Yingluoxia gaging station and the monthly groundwater level at the Minyong observation well were shown in two chart views.

Independent information for crosschecking and interpreting modeling results can also be visualized. In Tian et al. (2015b), ET data derived from remote sensing (RS) products (Wu et al., 2012) were compared against ET simulated by the GSFLOW model. RS products of LAI (Liao et al., 2013) also effectively assisted the interpretation of spatial and temporal patterns of hydrological simulations. Fig. 5c displays the ET field (1 km × 1 km grids) in a certain month, and the chart view exhibits the variability of monthly ET at the flagged location. Note that this ET data set does not cover the Badain Jaran Desert. Similarly, Fig. 5d displays the LAI field (1 km × 1 km grids) on a certain day, as well as the variability of daily-scale (one data point available in every eight days) LAI at the flagged location.

3.3. Visualization of model structures

IHM3D can also conveniently visualize the spatial delineation of an integrated SW–GW model. For example, the GSFLOW model in Tian et al. (2015b) used uniform 1 km × 1 km grids for both of

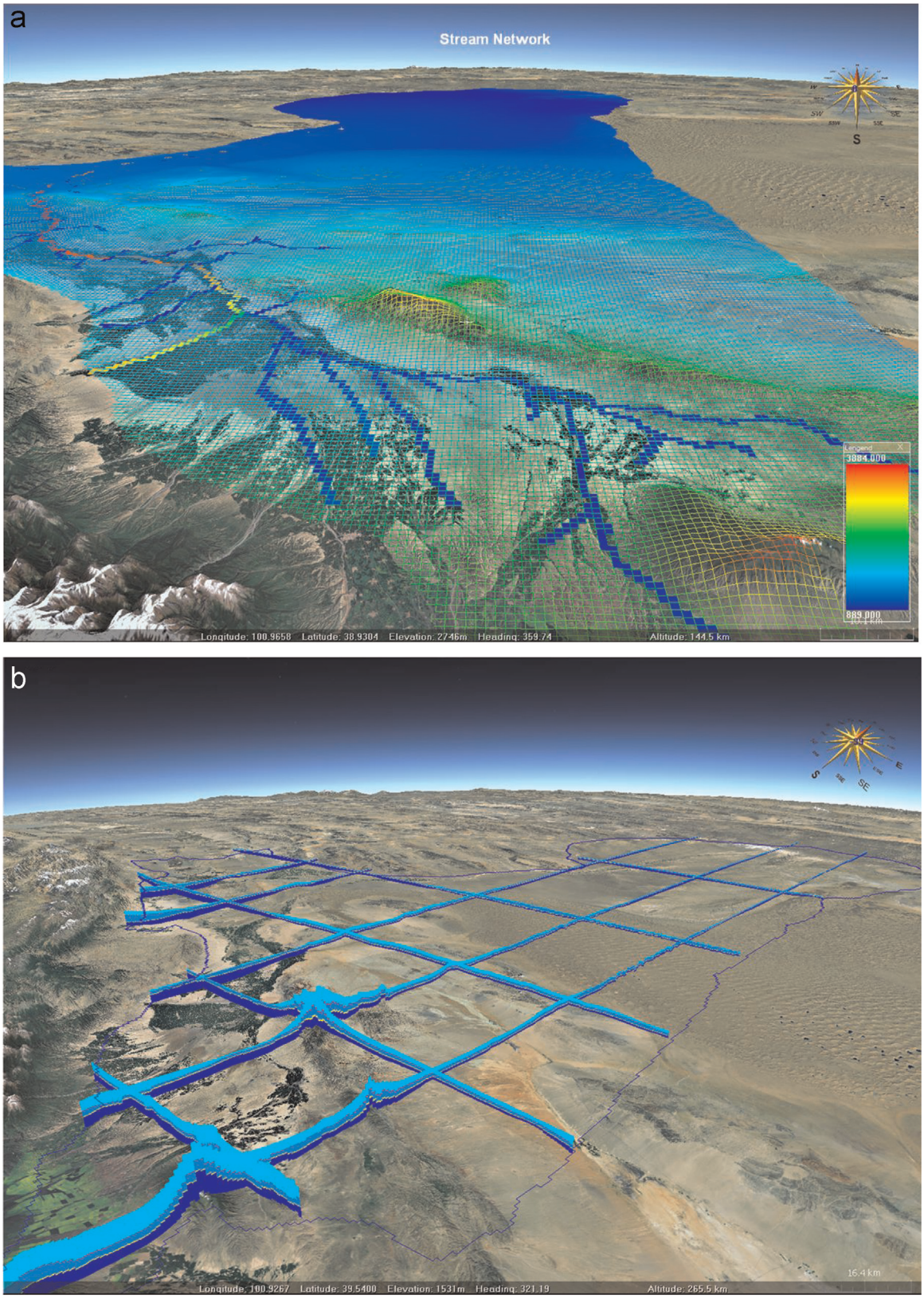

Fig. 7. Model structures. (a) 1 km × 1 km model grids and stream network; and (b) cross sections of the subsurface domain.

the surface and subsurface domains, as shown in Fig. 7a. Fig. 7a also displays the stream network, which is comprised of 3119 reaches. A reach is a section of stream that intersects a particular MODFLOW grid cell. The subsurface domain was divided into 5 layers. The first layer represents a shallow unconfined aquifer, the second and fourth layers represent aquitards, and the third and fifth layers represent a shallow confined aquifer and a deep confined aquifer, respectively. In IHM3D, by adding a hot point, the two aquifer cross-sections along the point's row and column can be visualized. Fig. 6b illustrates the cross-sections after selecting

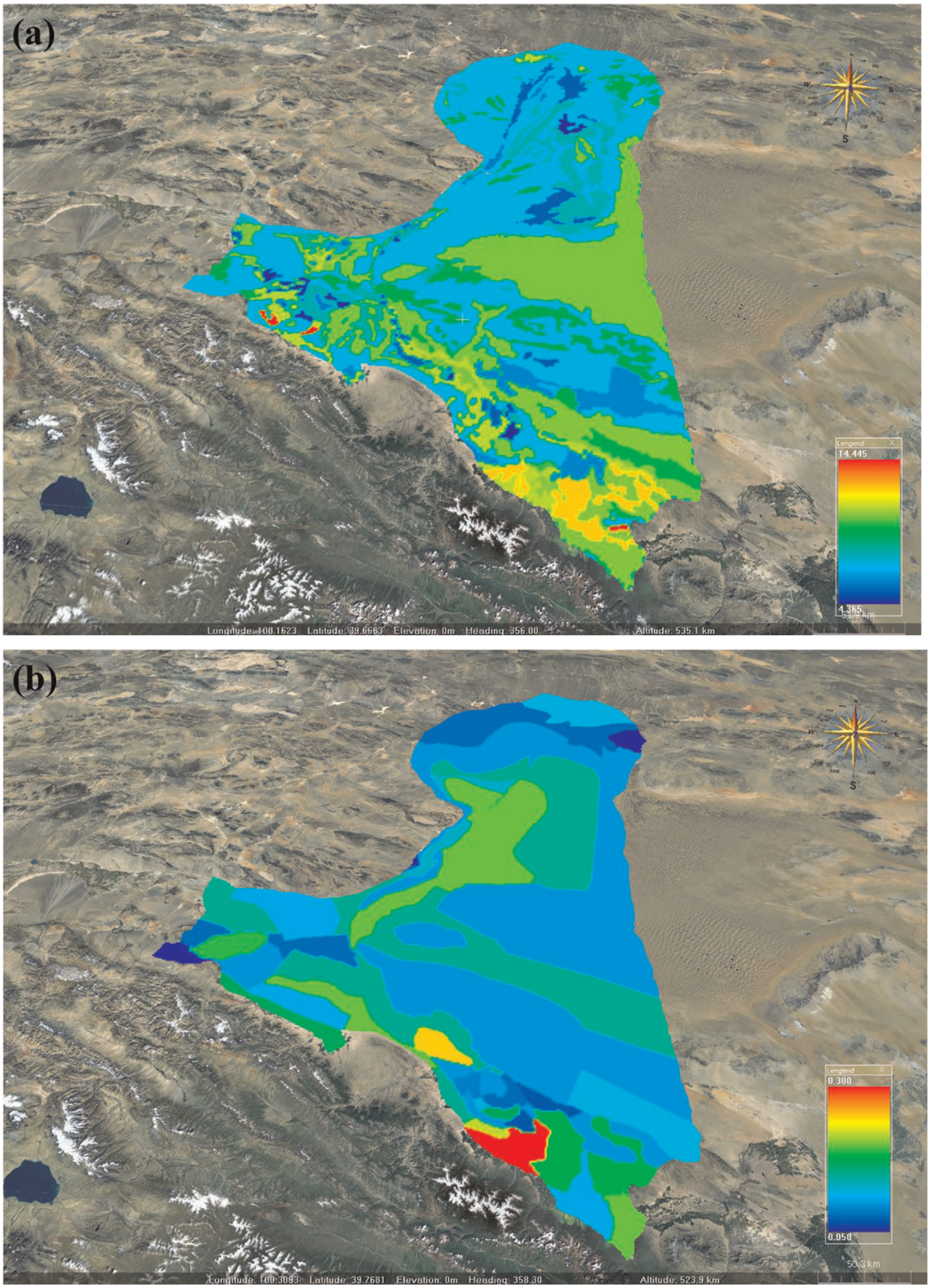

Fig. 8. Distributed model parameter values. (a) Soil's maximum available capillary water-holding capacity; and (b) specific yield for the top layer of aquifers.

multiple hot points. In the cross-sections, bands with different colors indicate different subsurface layers.

3.4. Visualization of distributed parameter values

IHM3D allows users to view all spatially distributed model parameters. By selecting a parameter name, the grid-based parameter values will be presented via different color ramps. Fig. 8a and b provide two examples: one is maximum available capillary water holding capacity of soil zone (a key HRU parameter), and the other is specific yield for the top subsurface layer.

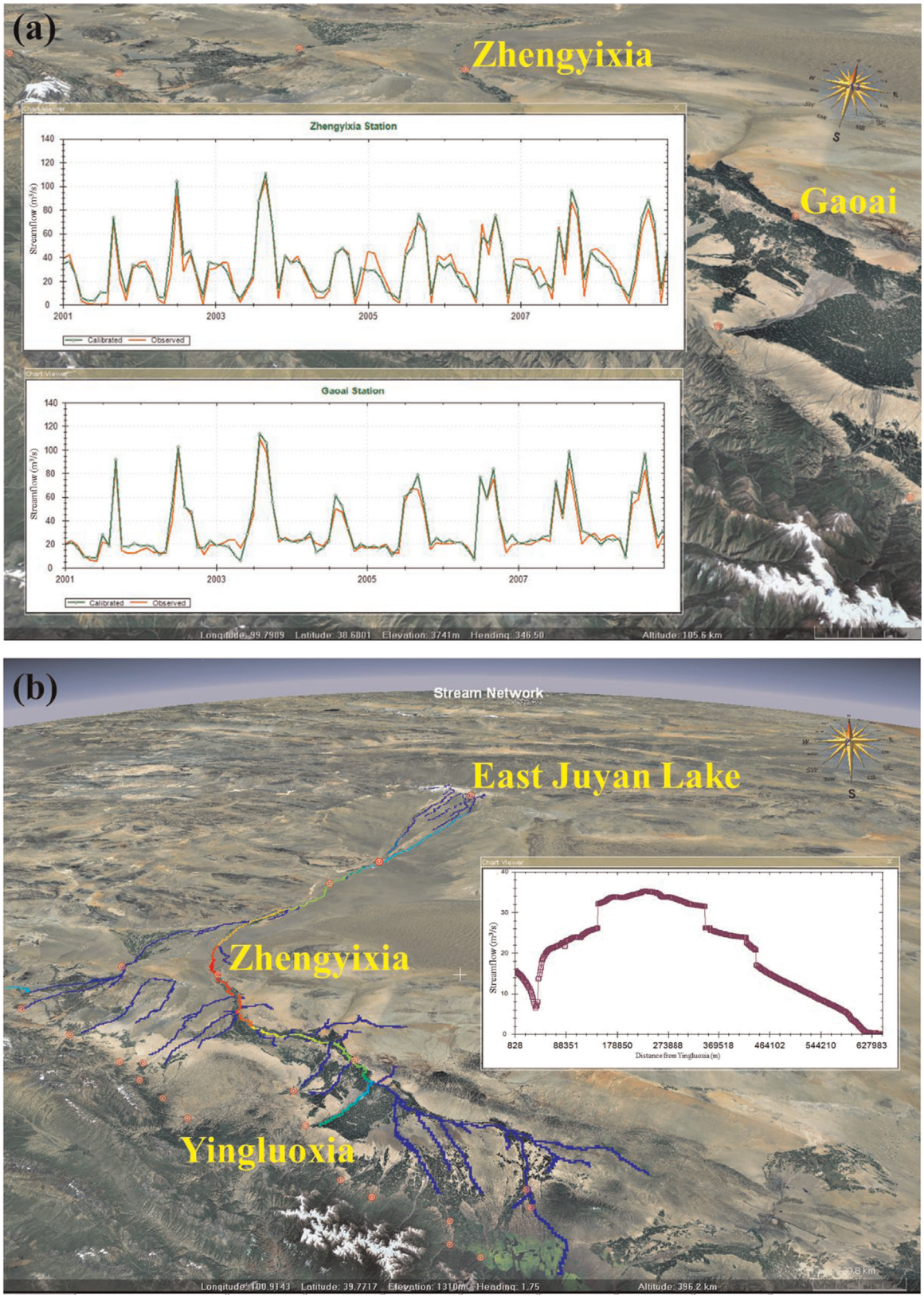

Fig. 9. Streamflow modeled by GSFLOW. (a) Comparison between the simulated streamflow and the observed streamflow at two gaging stations; and (b) spatial distribution of flow rate in the stream network.

3.5. *Visualization of model outputs*

An integrated SW–GW model typically generates a number of variables in diverse data structures. IHM3D was designed to streamline the entire procedure of withdrawing, processing and visualizing output data of integrated SW–GW models. With some simple operations, modeling results can be directly loaded from GSFLOW output files, processed and then displayed in the 3D

environment. A great amount of manual data processing efforts are then saved. IHM3D allows users to set a specific time span for the data presentation. Moreover, IHM3D can animate model outputs for the selected time span. Users are able to manipulate the animation through a controller which provides common operations like play, stop, pause, forward, and backward. As the output data are loaded into the computer memory, the system can provide fluent animation. In addition, the system is able to perform basic data analyses (e.g., deriving mean, sum, maximum and minimum values) for user-specified time periods and spatial

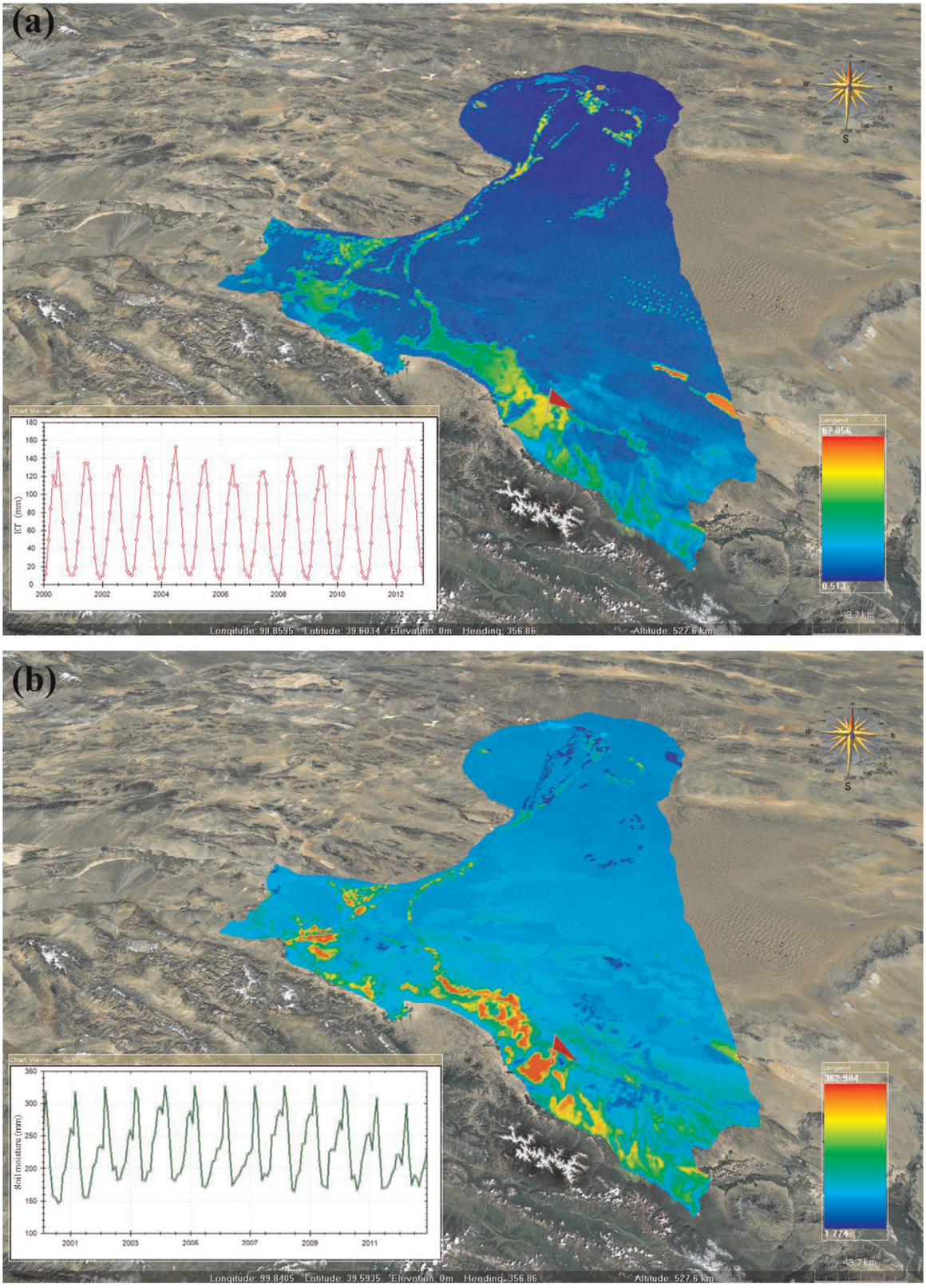

Fig. 10. Selected surface hydrology outputs. (a) Monthly evapotranspiration; and (a) monthly averaged soil moisture.

ranges. Some visualization examples are provided below.

Fig. 9a shows that IHM3D not only allows visualization of simulated streamflow at any reaches, but also enables a comparison of the simulated streamflow against the observed one at gaging stations. The observed streamflow data can be retrieved from the local database by IHM3D. This comparison functionality would greatly facilitate the model calibration and validation. Fig. 9b further visualizes the simulated daily flow rates in the entire stream network on a specific day, as well as the spatial variation of flow rate along the main river from Yingluoxia to East Juyan Lake (the

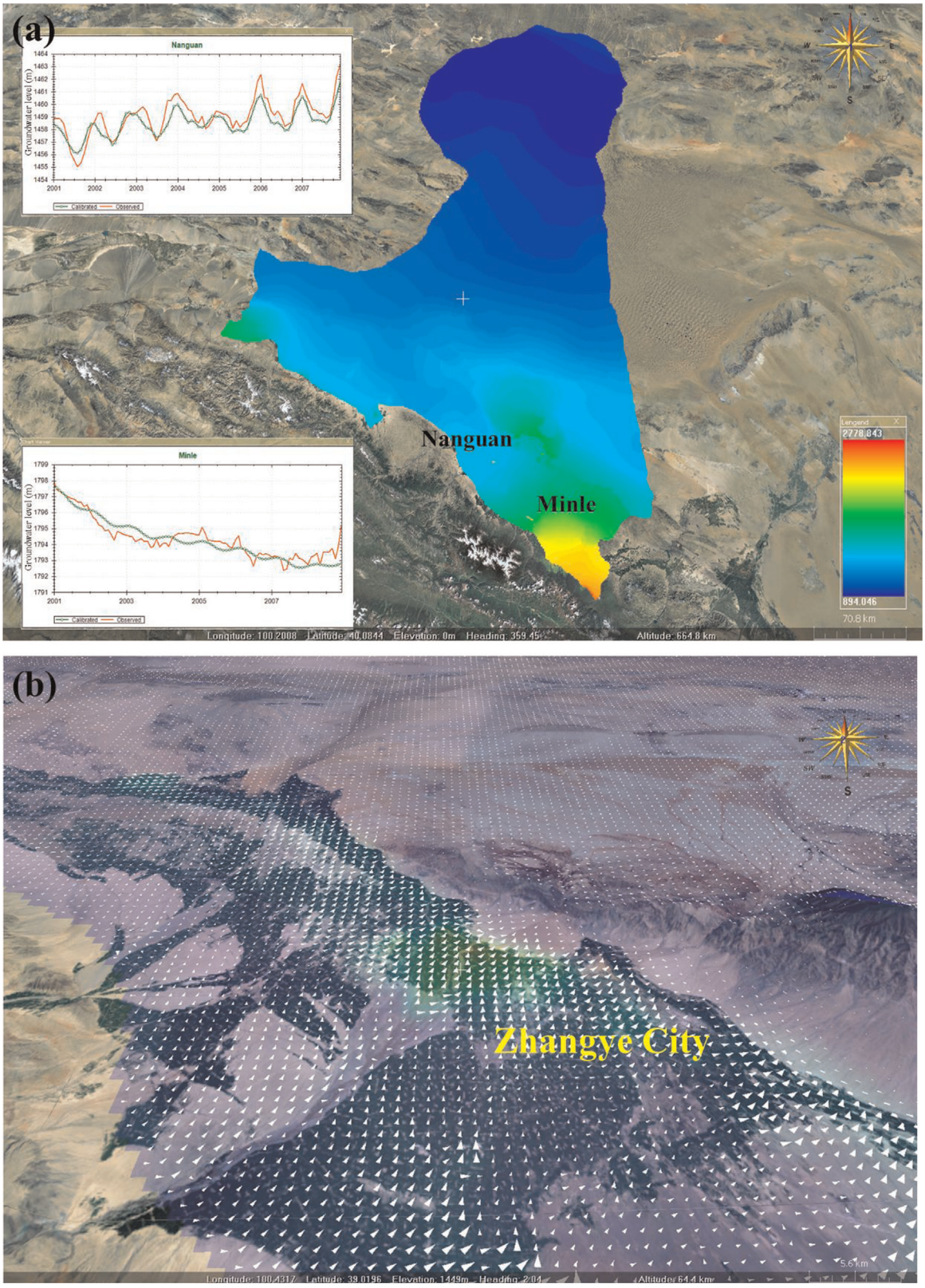

Fig. 11. Visualization of groundwater simulation results. (a) Spatial pattern of monthly averaged groundwater levels; and (b) groundwater velocity field.

chart view). This functionality is very useful in examining modeling results. For example, the sudden decreases and increases in the chart view of Fig. 8b actually indicate flow diversion and tributary inflow, respectively. IHM3D can illustrate stream-aquifer exchanges in the same manner (although not shown here), which would be of great importance to understanding the complex hydrological processes in this arid region.

Fig. 9a and b present the modeled ET and soil moisture fields in a specific month, respectively. The areas with high ET and soil moisture values in the middle HRB are intensively irrigated farmlands. Users can also examine time-series data at any locations within the modeling domain, as demonstrated by the chart views in Fig. 10.

Fig. 11a shows the spatial pattern of monthly average groundwater level in a selected month. The chart view compares the observed and simulated groundwater levels at two wells (i.e., Minle and Nanguan). It clearly indicates that the model has successfully reproduced the seasonal variation of groundwater level. In addition, IHM3D is able to plot velocity vectors as arrows to visualize direction and speed of groundwater flow. This useful functionality is also provided by commercial software like Visual MODFLOW. Fig. 11b displays a horizontal-plane view of velocity vectors. Each arrow is placed on the center of its corresponding grid cell. Users can change arrow styles (e.g., color schema) and scaling method. It can be seen from Fig. 11b that the fastest groundwater movement occurs around the edge of the alluvia fan near the Zhangye City, as indicated by the color of velocity filed (the warm-toned colors stand up faster velocity speed). Overall, Fig. 11 indicates that IHM3D can greatly help understand complex groundwater processes at a large basin scale.

4. Conclusions

In this study, we designed and developed a 3D visualization software, named IHM3D, streamlined for integrated SW–GW modeling. IHM3D enables to overlay geo-referenced data sets in a virtual 3D environment. It can effectively and efficiently visualize various types of model inputs and outputs in space and in time, without transforming them into standard GIS layers. The case study in the Heihe River Basin demonstrated the applicability of the software for integrated SW–GW modeling at a large basin scale. Visualization of the modeling results by GSLFOW greatly facilitates our understanding on the complicated hydrologic cycle in the study area, and provides insights into the regional water resources management. Overall, IHM3D can enhance the data and model sharing in the water resources research community, and makes the integrated SW–GW modeling more practical in supporting water resources management.

Although the current version of IHM3D was developed specifically for GSFLOW, it can be easily modified to suit other models, since GSFLOW has a representative data structure of integrated SW–GW models. In addition, as hydrologic and geoscience datasets continue to expand in size and scope, future developments may focus on improving the 3D rendering performance to display massive datasets. To this end, more advanced techniques such as volume rendering, tessellation, data and task parallelism within the visualization pipeline can be employed.

Software availability

IHM3D is free for non-commercial use. Anyone who is interested in testing or using the software can contact us at tiany@sustc.edu.cn or yizheng@pku.edu.cn to receive the software and a license key. Commercial users must purchase a license to use the software.

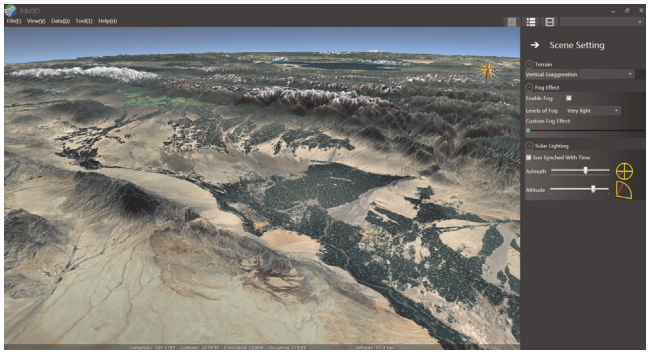

Video S1. Video demo of IHM3D.A video clip is available online.Supplementary material related to this article can be found online at http://dx.doi.org/10.1016/j.cageo.2015.09.019.

Acknowledgments

We are grateful to the funding support from the National Natural Science Foundation of China (NSFC) (Nos. 91225301; 91125021) and China's National Science & Technology Pillar Program (No. 2012BAC03B02). The data used in the application case were provided by the Heihe Program Data Management Center (http://www.heihedata.org).

Appendix A. Supplementary material

The following are the supplementary data to this article: Video S1.

References

Ames, D.P., Horsburgh, J.S., Cao, Y., Kadlec, J., Whiteaker, T., Valentine, D., 2012. HydroDesktop: web services-based software for hydrologic data discovery, download, visualization, and analysis. Environ. Model. Softw. 37, 146–156.
Bae, D.-H., Jung, I.-W., Lettenmaier, D.P., 2011. Hydrologic uncertainties in climate change from IPCC AR4 GCM simulations of the Chungju Basin, Korea. J. Hydrol. 401 (1–2), 90–105.
Bernardin, T., Cowgill, E., Kreylos, O., Bowles, C., Gold, P., Hamann, B., Kellogg, L., 2011. Crusta: a new virtual globe for real-time visualization of sub-meter digital topography at planetary scales. Comput. Geosci. 37, 75–85.
Brooks, S., Whalley, J.L., 2008. Multilayer hybrid visualizations to support 3D GIS. Comput. Environ. Urban Syst. 32, 278–292.
Brunner, P., Simmons, C.T., 2012. HydroGeoSphere: a fully integrated, physically based hydrological model. Ground Water 50, 170–176.
Boschetti, L., Roy, D.P., Justice, C.O., 2008. Using NASA's World Wind virtual globe for interactive internet visualization of the global MODIS burned area product. Int. J. Remote Sens. 29, 3067–3072.
Castrillón, M., Jorge, P.A., López, I.J., Macías, A., Martín, D., Nebot, R.J., Sabbagh, I., Quintana, F.M., Sánchez, J., Sánchez, A.J., Suárez, J.P., Trujillo, A., 2011. Forecasting and visualization of wildfires in a 3D geographical information system. Comput. Geosci. 37, 390–396.
Chen, A., Leptoukh, G., Kempler, S., Lynnes, C., Savtchenko, A., Nadeau, D., Farley, J., 2009. Visualization of A-train vertical profiles using Google Earth. Comput. Geosci. 35, 419–427.
Gilfedder, M., Rassam, D.W., Stenson, M.P., Jolly, I.D., Walker, G.R., Littleboy, M., 2012. Incorporating land-use changes and surface–groundwater interactions in a simple catchment water yield model. Environ. Model. Softw. 38, 62–73.
Condon, L.E., Maxwell, R.M., 2013. Implementation of a linear optimization water allocation algorithm into a fully integrated physical hydrology model. Adv. Water Resour. 60 (0), 135–147.
Graham, D.N., Butts, M.B., 2005. Flexible, integrated watershed modelling with MIKE SHE. In: Singh, V.P., Frevert, D.K. (Eds.), Watershed Models. CRC Press, USA, pp. 245–272.
Hassan, S.M.T., Lubczynski, M.W., Niswonger, R.G., Su, Z., 2014. Surface–groundwater interactions in hard rocks in Sardon Catchment of western Spain: an integrated modeling approach. J. Hydrol. 517, 390–410.
Hirschi, M.B., Mueller, W.D., Seneviratne, S.I., 2014. Using remotely sensed soil moisture for land–atmosphere coupling diagnostics: the role of surface vs. root-zone soil moisture variability. Remote Sens. Environ. 154 (0), 246–252.
Horsburgh, J.S., Tarboton, D.G., Maidment, D.R., Zaslavsky, I., 2008. A relational model for environmental and water resources data. Water Resour. Res. 44 (5), W05406. http://dx.doi.org/10.1029/2007WR006392.

Horsburgh, J.S., Reeder, S.L., 2014. Data visualization and analysis within a hydrologic information system: integrating with the R statistical computing environment. Environ. Model. Softw. 52, 51–61.
Huang, M., Tian, Y., 2013. A novel visual modeling system for time series forecast: application to the domain of hydrology. J. Hydroinform. 15 (1), 21–37.
Hu, R., Yan, G., Mu, X., Luo, J., 2014. Indirect measurement of leaf area index on the basis of path length distribution. Remote Sens. Environ. 155, 239–247.
Huntington, J.L., Niswonger, R.G., 2012. Role of surface-water and groundwater interactions on projected summertime streamflow in snow dominated regions: an integrated modeling approach. Water Resour. Res. 48, W11524. http://dx.doi.org/10.1029/2012WR012319.
Jacobson, A., Dhanota, J., Godfrey, J., Jacobson, H., Rossman, Z., Stanish, A., Walker, H., Riggio, J., 2015. A novel approach to mapping land conversion using Google Earth with an application to East Africa. Environ. Model. Softw. 72, 1–9.
Jiao, J.J., Zhang, X., Wang, X., 2015. Satellite-based estimates of groundwater depletion in the Badain Jaran Desert, China. Sci. Rep. 5, 8960. http://dx.doi.org/10.1038/srep08960.
Kühnlein, M., Appelhans, T., Thies, B., Nauss, T., 2014. Improving the accuracy of rainfall rates from optical satellite sensors with machine learning—a random forests-based approach applied to MSG SEVIRI. Remote Sens. Environ. 141, 129–143.
Lázaro, M., Navarro, J., Gil, A., Romero, V., 2014. 3D-geological structures with digital elevation models using GPU programming. Comput. Geosci. 70, 138–146.
Leavesley, G.H., Lichty, R.W., Troutman, B.M., Saindon, L.G., 1983. Precipitation-runoff Modeling System: User's Manual. USGS Water-Resources Investigations Report: 83e4238, 206 pp. Available at: ⟨http://pubs.usgs.gov/wri/1983/4238/report.pdf⟩.
Li, J., Jiang, Y., Yang, C., Huang, Q., Rice, M., 2013. Visualizing 3D/4D environmental data using many-core graphics processing units (GPUs) and multi-core central processing units (CPUs). Comput. Geosci. 59, 78–89.
Liao, Y., Fan, W., Xu, X., 2013. Algorithm of Leaf Area Index product for HJ-CCD over Heihe River Basin. In: Proceedings of the 2013 IEEE International Geoscience and Remote Sensing Symposium (IGARSS). pp. 169–172.
Lindstrom, P., Koller, D., Ribarsky, W., Hodges, L.F., Faust, N., Turner, G.A., 1996. Real-time, continuous level of detail rendering of height fields. In: Proceedings of the 23rd Annual Conference on Computer Graphics and Interactive Techniques. ACM, pp. 109–118.
Liu, P., Gong, J., Yua, M., 2015. Visualizing and analyzing dynamic meteorological data with virtual globes: a case study of tropical cyclones. Environ. Model. Softw. 64, 80–93.
Markstrom, S.L., 2012. Integrated Watershed-scale Response to Climate Change for Selected Basins Across the United States. U.S. Geology Survey Scientific Investigations Reports 2011–5077.143 pp.
Markstrom, S.L., Niswonger, R.G., Regan, R.S., Prudic, D.E., Barlow, P.M., 2008. GSFLOW-Coupled Ground-water and Surface-water FLOW model based on the integration of the Precipitation-Runoff Modeling System (PRMS) and the Modular Ground-Water Flow Model (MODFLOW-2005). U.S. Geological Survey Techniques and Methods 6–D1. 240 pp.
Maxwell, R.M., Kollet, S.J., 2008. Interdependence of groundwater dynamics and land-energy feedbacks under climate change. Nat. Geosci. 1, 665–669.
Maxwell, R.M., Putti, M., Meyerhoff, S., Delfs, J.-O., Ferguson, I.M., Ivanov, V., Kim, J., Kolditz, O., Kollet, S.J., Kumar, M., Lopez, S., Niu, J., Paniconi, C., Park, Y.-J., Phanikumar, M.S., Shen, C., Sudicky, E.A., Sulis, M., 2014. Surface-subsurface model intercomparison: a first set of benchmark results to diagnose integrated hydrology and feedbacks. Water Resour. Res. 50, 1531–1549.
Merritt, M.L., Konikow, L.F., 2000. Documentation of a Computer Program to Simulate Lake–Aquifer Interaction Using the MODFLOW Ground Water Flow Model and the MOC3D Solute-Transport Model. U.S. Geological Survey Water-Resources Investigations Report 2000-4167, 146 pp. Available at: ⟨https://water.usgs.gov/nrp/gwsoftware/modflow2000/wri00_4167.pdf⟩.
Michaelis, C., Ames, D., 2012. Considerations for implementing OGC WMS and WFS specifications in a desktop GIS. J. Geogr. Inf. Syst. 4 (2), 161–167.
McCarthy, J.D., Graniero, P.A., 2006. A GIS-based borehole data management and 3D visualization system. Comput. Geosci. 32, 1699–1708.
Mochales, T., Blenkinsop, T.G., 2014. Representation of paleomagnetic data in virtual globes: a case study from the Pyrenees. Comput. Geosci. 70, 56–62.
Niswonger R.G., Prudic D.E. and Regan R.S., 2006. Documentation of the Unsaturated-Zone Flow (UZF1) Package for Modeling Unsaturated Flow Between the Land Surface and the Water Table with MODFLOW-2005, U.S. Geological Survey Techniques and Methods 6-A19, 62 pp. Available at: ⟨http://pubs.usgs.gov/tm/2006/tm6a19/pdf/tm6a19.pdf⟩.
Niswonger, R.G., Prudic, D.E., 2010. Documentation of the Streamflow-Routing (SFR2) Package to Include Unsaturated Flow Beneath Streams—A Modification to SFR1. U.S. Geological Survey Techniques and Methods 6-A13, 50 pp. Available at: ⟨http://pubs.usgs.gov/tm/2006/tm6A13/pdf/tm6a13.pdf⟩.
Osna, T., Sezer, E.A., Akgun, A., 2014. GeoFIS: an integrated tool for the assessment of landslide susceptibility. Comput. Geosci. 66, 20–30.
Peckham, S.D., Goodall, J.L., 2013. Driving plug-and-play models with data from web services: a demonstration of interoperability between CSDMS and CUAHSI-HIS. Comput. Geosci. 53 (0), 154–161.
Pérez, A.J., Abrahão, R., Causapé, J., Cirpka, O.A., Bürger, C.M., 2011. Simulating the transition of a semi-arid rainfed catchment towards irrigation agriculture. J. Hydrol. 409, 663–681.
Rasmussen, M.O., Sørensen, M.K., Wu, B., Yan, N., Qin, H., Sandholt, I., 2014. Regional-scale estimation of evapotranspiration for the North China Plain using MODIS data and the triangle-approach. Int. J. Appl. Earth Obs. Geoinform. 31, 143–153.
Shen, C., Phanikumar, M.S., 2010. A process-based, distributed hydrologic model based on a large-scale method for surface–subsurface coupling. Adv. Water Resour. 33, 1524–1541.
Shojaei, D., Kalantari, M., Bishop, I.D., Rajabifard, A., Aien, A., 2013. Visualization requirements for 3D cadastral systems. Comput. Environ. Urban Syst. 41, 39–54.
Srivastava, V., Graham, W., Muñoz-Carpena, R., Maxwell, R.M., 2014. Insights on geologic and vegetative controls over hydrologic behavior of a large complex basin – global sensitivity analysis of an integrated parallel hydrologic model. J. Hydrol. Part B 519, 2238–2257.
Steiniger, S., Hunter, A.J.S., 2013. The 2012 free and open source GIS software map – a guide to facilitate research, development, and adoption. Comput. Environ. Urban Syst. 39, 136–150.
Suárez, J.P., Plaza, A., 2009. Four-triangles adaptive algorithms for RTIN terrain meshes. Math. Comput. Model. 49, 1012–1020.
Surfleet, C.G., Tullos, D., Chang, H., Jung, I.-W., 2012. Selection of hydrologic modeling approaches for climate change assessment: a comparison of model scale and structures. J. Hydrol. 464–465 (0), 233–248.
Tian, Y., Zheng, Y., Wu, B., Wu, X., Liu, J., Zheng, C., 2015a. Modeling surface water–groundwater interaction in arid and semi-arid regions with intensive agriculture. Environ. Model. Softw. 63, 170–184.
Tian, Y., Zheng, Y., Zheng, C., Xiao, H., Fang, J., Zou, S., Wu, B., Yao, Y., Zhang, A., Liu, J., 2015b. Exploring scale-dependent ecohydrological responses in a large endorheic river basin through integrated surface water–groundwater modeling. Water Resour. Res. 51 (6), 4065–4085.
Wang, Y., Huynh, G., Williamson, C., 2013. Integration of Google Maps/Earth with microscale meteorology models and data visualization. Comput. Geosci. 61, 23–31.
Wu, B., Yan, N., Xiong, J., Bastiaanssen, W.G.M., Zhu, W., Stein, A., 2012. Validation of ETWatch using field measurements at diverse landscapes: a case study in Hai Basin of China. J. Hydrol. 436–437, 67–80.
Wu, B., Zheng, Y., Tian, Y., Wu, X., Yao, Y., Han, F., Liu, J., Zheng, C., 2014. Systematic assessment of the uncertainty in integrated surface water–groundwater modeling based on the probabilistic collocation method. Water Resour. Res. 50 (7), 5848–5865.
Wu, B., Zheng, Y., Wu, X., Tian, Y., Han, F., Liu, J., Zheng, C., 2015. Optimizing water resources management in large river basins with integrated surface water–groundwater modeling: a surrogate-based approach. Water Resour. Res. 51 (4), 2153–2173. http://dx.doi.org/10.1002/2014WR016653.
Wu, H., He, Z., Gong, J., 2010. A virtual globe-based 3D visualization and interactive framework for public participation in urban planning processes. Comput. Environ. Urban Syst. 34, 291–298.
Xiong, Z., Fu, C., Yan, X., 2009. Regional integrated environmental model system and its simulation of East Asia summer monsoon. Chin. Sci. Bull. 54, 4253–4261.
Xiong, Z., Yan, X., 2013. Building a high-resolution regional climate model for the Heihe River Basin and simulating precipitation over this region. Chin. Sci. Bull. 58 (36), 4670–4678.
You, H., Kim, D., Seo, Y., 2014. HydroConnector: a tool for estimating stage height of ungaged river site based on standardized hydro web services and HPG model. Comput. Geosci. 70 (0), 73–79.
Zhu, L., Wang, X., Zhang, B., 2014. Modeling and visualizing borehole information on virtual globes using KML. Comput. Geosci. 62, 62–70.